

## Internal amplitude, structure and identification of CAEs and GAEs in NSTX\* EX-W

N. A. Crocker, E. D. Fredrickson<sup>1</sup>, N. N. Gorelenkov<sup>1</sup>, W. A. Peebles, S. Kubota, R. E. Bell<sup>1</sup>, B. P. LeBlanc<sup>1</sup>, J. E. Menard<sup>1</sup>, M. Podestà<sup>1</sup>, K. Tritz<sup>2</sup> and H. Yuh<sup>3</sup>

Univ. of California, Los Angeles, CA 90095

<sup>1</sup>Princeton Plasma Physics Laboratory, Princeton New Jersey 08543

<sup>2</sup>The Johns Hopkins University, Baltimore, MD 21218, USA

<sup>3</sup>Nova Photonics, Princeton, NJ 08543

Email contact of main author: ncrocker@physics.ucla.edu

Fast-ions (e.g. fusion alphas and neutral beam ions) will excite a wide range of instabilities in ITER. Among the possible instabilities are high frequency compressional (CAE) and global (GAE) Alfvén eigenmodes excited through Doppler-shifted cyclotron resonance with beam ions [1]. Modes identified as GAEs have previously been demonstrated to cause fast-ion transport [2,3] and to potentially play a role in electron thermal transport [4]. Modes identified as CAEs have been postulated to contribute to ion heating [5]. The impact on plasma performance of CAEs and GAEs is investigated in NSTX. This is facilitated by a recently upgraded array of 16 fixed-frequency quadrature reflectometers. Detailed measurements of CAE and GAE amplitude and eigenmode structure were obtained in a high power (6 MW), beam-heated H-mode plasma (shot 141398) [6] (Fig. 1) very similar to those discussed in Ref. [4]. These measurements, which extend from the plasma edge to deep in the core, can be used in modeling the effects of the modes on electron thermal transport. The observed modes are identified by comparison of their frequency and measured toroidal mode numbers with local Alfvén dispersion relations [6] (Fig. 2). The modes identified as CAEs have higher frequencies and smaller toroidal mode numbers (i.e. smaller  $|n|$ ) than the GAEs. Also, they are strongly core localized, in contrast with the GAEs, which also peak toward the plasma center but have much broader radial extent. Identification of the modes can aid in predicting their impact on fast-ion and electron transport, as well as ion heating, since CAEs and GAEs are expected to have very different effects on particle orbits.

CAE and GAE amplitude and eigenmode structure are measured using a recently upgraded array of reflectometers, with frequencies spread over 30 – 75 GHz, corresponding to cutoff densities of  $1.1 - 6.9 \times 10^{13} \text{ cm}^{-3}$  when operating with ordinary-mode polarization [6]. The array provides a radially distributed set of localized density fluctuation measurements. Figure 1b shows the magnitude of the *effective displacement* ( $\xi = \delta\phi/2k_0$ ) vs. cutoff radius for a spectrum (Fig. 1a) of the observed modes at the deepest measurement location,  $R = 1.16 \text{ m}$ . (The magnetic axis is at  $R_0 = 1.05 \text{ m}$ .) The effective displacement ( $\xi$ ), determined from the reflectometer phase fluctuation ( $\delta\phi$ ) and the vacuum microwave wavenumber ( $k_0$ ), approximates the displacement of the cutoff density location for global modes with large radial extent [7]. As can be seen in Fig. 1c, which shows  $|\xi|$  vs.  $R$ , normalized by  $|\xi|$  at  $R = 1.16 \text{ m}$ , the modes can be divided into two categories based on frequency and structure. Modes with  $f > \sim 600 \text{ kHz}$  tend to be strongly localized to the core ( $R < \sim 1.3 \text{ m}$ ), while the modes at lower frequency tend to have more radially extended structure, peaking toward the magnetic axis, but with significant amplitude at the plasma edge. The peaking of all the modes in the core is significant because it is a key factor motivating the postulated role of the modes in electron thermal transport [4].

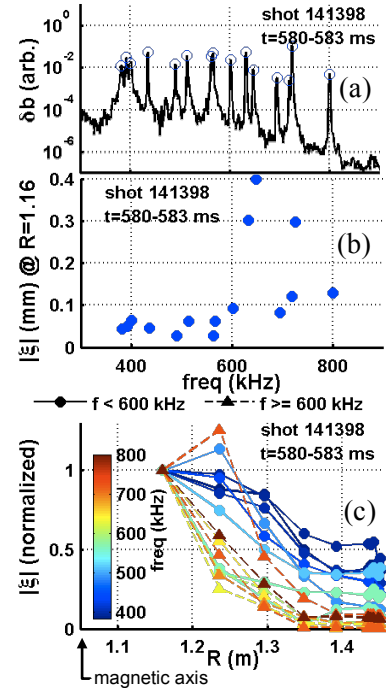


**Figure 1:** (a)  $\delta b$  spectrum with modes marked; (b) Effective radial displacement ( $|\xi|$ ) of modes at  $R=1.16 \text{ m}$ ; and (c)  $|\xi|$  vs.  $R$ , normalized by  $|\xi|$  at  $R=1.16 \text{ m}$ .

The two groups of modes also have distinctly different ranges of toroidal mode number,  $n$ . Toroidal mode numbers are obtained from an irregularly toroidally distributed array of twelve magnetic sensing coils with separations ranging from  $10^\circ$  to  $180^\circ$  that allows  $|n|$  as high as 18 to be distinguished. The  $f > \sim 600$  kHz modes have  $n = -3, -4$  and  $-5$ . In contrast, the  $f < \sim 600$  kHz modes have larger mode numbers,  $n = -6, -7, -8$ . All of the modes propagate counter to the neutral beams, consistent with excitation by Doppler-shifted cyclotron resonance with beam ions ( $f_{cyclotron} = 2.4$  MHz) [8].

To identify the modes shown in Fig. 1, frequency and toroidal mode number (Fig. 2a) are used in conjunction with local Alfvén dispersion relations [6]. For instance, the CAE local dispersion relationship,  $\omega^2 \sim k^2 V_A^2$ , can be used to establish minimum requirements on  $\omega$  and  $n$  for CAEs. For  $n \neq 0$ , CAEs are confined within a "well" in the  $R$ - $Z$  plane where  $\omega^2 - (n^2/R^2)V_A^2 > 0$ . Inside the well, compressional Alfvén waves propagate, but are evanescent outside. Of course, the  $R$ - $Z$  "wavelength",  $\lambda_{R-Z} = (\omega^2/V_A^2 - n^2/R_0^2)^{-1/2}/2\pi$ , should be smaller than the well. The modes are compared with these expectations using equilibrium electron density from Multipoint Thomson Scattering and the magnetic field from equilibrium reconstruction by the LRDFIT code. The Doppler shift due to toroidal rotation is also compensated using plasma rotation from Charge Exchange Recombination Spectroscopy. Because of their smaller  $n$ , the  $f > \sim 600$  kHz modes easily meet the requirements. In contrast, the  $f < \sim 600$  kHz modes range from having  $\omega^2 - (n^2/R_0^2)V_A^2 < 0$  at the lowest frequencies to having  $\lambda_{R-Z} > \sim R_0$  at the highest frequencies. Comparison of long-term mode frequency evolution (Fig. 2a) with expectation for GAEs also proves informative. GAEs peak near a minimum of the Alfvén continuum (e.g. at the magnetic axis) and have frequencies  $\omega \sim |k_{||}|V_A$ , where  $k_{||} \approx (m/q-n)/R$ . The modes in Fig. 1 peak near the magnetic axis, so the GAE frequency is calculated using safety factor ( $q_0$ ), Alfvén frequency ( $f_{A0} = V_{A0}/2\pi R_0$ ) and toroidal rotation ( $f_{ROTO}$ ) (Fig. 2b) evaluated at the magnetic axis. Figure 2c illustrates an example of the analysis for the  $f = 633$  kHz mode, showing that the mode frequency appears to evolve inconsistently with the GAE frequency. This is largely due to a high sensitivity to  $q_0$  variation. The low  $|n|$  mandates a large poloidal mode number,  $m$ , to fit the observed frequency. The frequencies of the other  $f > \sim 600$  kHz modes also evolve inconsistently with the GAE frequency. In contrast, the lower frequency modes have a frequency evolution consistent with the expectation for a GAE. They tend to have high  $|n|$ , leading to low  $m$ , so the expected GAE frequency is relatively insensitive to  $q_0$  variation.

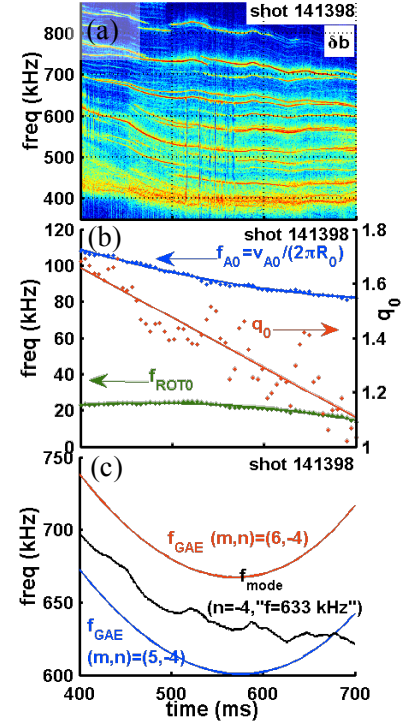


**Figure 2:** (a)  $\delta b$  spectrum with CAEs and GAEs; (b) Equilib. parameters at magn. axis: Alfvén frequency ( $f_{A0}$ ), toroidal rotation ( $f_{ROTO}$ ) and safety factor ( $q_0$ ); and (c) frequency of " $f = 633$  kHz" mode (cf. Fig. 1) compared with GAE frequency.

Figure 2c illustrates an example of the analysis for the  $f = 633$  kHz mode, showing that the mode frequency appears to evolve inconsistently with the GAE frequency. This is largely due to a high sensitivity to  $q_0$  variation. The low  $|n|$  mandates a large poloidal mode number,  $m$ , to fit the observed frequency. The frequencies of the other  $f > \sim 600$  kHz modes also evolve inconsistently with the GAE frequency. In contrast, the lower frequency modes have a frequency evolution consistent with the expectation for a GAE. They tend to have high  $|n|$ , leading to low  $m$ , so the expected GAE frequency is relatively insensitive to  $q_0$  variation.

\*Work supported by U.S. DOE Contracts DE-FG02-99ER54527 and DE-AC02-09CH11466.

- 
- [1] W.W. Heidbrink, *et al.*, *Nucl. Fusion* **46**, 324 (2006).
  - [2] E. D. Fredrickson, *et al.*, *Europhys. Conf. Abstracts* **35G**, P2.119 (2011).
  - [3] E. D. Fredrickson, *et al.*, Proc. of the 23rd IAEA Fusion Energy Conf., Daejon, Korea Rep. of, 11-16 October 2010, EXW/P7-06-1-8 (2011).
  - [4] Stutman D, *et al.*, *Phys. Rev. Lett.* **102**, 115002 (2009).
  - [5] D. Gates, R. White, and N. Gorelenkov, *Phys. Rev. Lett.* **87**, 205003 (2001).
  - [6] N. A. Crocker, *et al.*, *Plasma Phys. Controll. Fusion* **15**, 105001 (2011).
  - [7] R. Nazikian, G. J. Kramer, and E. Valeo, *Phys. Plasmas* **8**, 1840 (2001).
  - [8] N. N. Gorelenkov, *et al.*, *Nucl. Fusion* **4**, 3228 (2003).